^{18}F-FDG PET/CT and ^{123}I-Metaiodobenzylguanidine Imaging in High-Risk Neuroblastoma: Diagnostic Comparison and Survival Analysis

Nikolaos D. Papathanasiou[1], Mark N. Gaze[2], Kevin Sullivan[2], Matthew Aldridge[1], Wendy Waddington[1], Ahmad Almuhaideb[1], and Jamshed B. Bomanji[1]

[1]*Institute of Nuclear Medicine, University College London Hospital, London, United Kingdom; and* [2]*Radiotherapy Department, University College London Hospital, London, United Kingdom*

The aim of our study was to evaluate prospectively the diagnostic performance and prognostic significance of ^{18}F-FDG PET/CT in comparison with ^{123}I-metaiodobenzylguanidine (^{123}I-MIBG) imaging in patients with high-risk neuroblastoma. **Methods:** Twenty-eight patients with refractory or relapsed high-risk neuroblastoma (16 male and 12 female patients; age range, 2–45 y; median age, 7.5 y) were simultaneously evaluated with ^{18}F-FDG PET/CT and ^{123}I-MIBG imaging before treatment with high-dose ^{131}I-MIBG. We compared the 2 methods in mapping tumor load, according to the extent of disease and intensity of positive lesions identified in each patient. Separate comparisons were performed for the soft-tissue and bone–bone marrow components of tumor burden. Survival analysis was performed to assess the prognostic significance of ^{18}F-FDG and ^{123}I-MIBG imaging parameters. **Results:** ^{18}F-FDG PET/CT results were positive in 24 of 28 (86%) patients, whereas ^{123}I-MIBG imaging results were positive in all patients. ^{18}F-FDG was superior in mapping tumor load in 4 of 28 (14%) patients, whereas ^{123}I-MIBG was better in 12 of 28 (43%) patients. In the remaining 12 (43%) patients, no major differences were noted between the 2 modalities. ^{18}F-FDG PET/CT missed 5 cases of bone–bone marrow disease, 4 cases of soft-tissue disease, and 6 cases of skull involvement that were positive on ^{123}I-MIBG scans. Cox regression and Kaplan–Meier survival curves showed that the group of patients (4/28) in whom ^{18}F-FDG was superior to ^{123}I-MIBG had a significantly lower survival rate than the others. Tumoral avidity for ^{18}F-FDG (maximum standardized uptake value) and extent of ^{18}F-FDG–avid bone–bone marrow disease were identified as adverse prognostic factors. **Conclusion:** ^{123}I-MIBG imaging is superior to ^{18}F-FDG PET/CT in the assessment of disease extent in high-risk neuroblastoma. However, ^{18}F-FDG PET/CT has significant prognostic implications in these patients.

Key Words: neuroblastoma; positron emission tomography; ^{18}F-fluorodeoxyglucose (^{18}F-FDG); ^{123}I-metaiodobenzylguanidine (^{123}I-MIBG)

J Nucl Med 2011; 52:519–525
DOI: 10.2967/jnumed.110.083303

More than half of patients with neuroblastoma are defined as high risk according to unfavorable prognostic features such as age (≥18 mo at presentation), stage (distant metastases in lymph nodes, cortical bone, bone marrow, and liver), and molecular pathology (MYCN oncogene amplification) (*1*). These patients require multimodality treatment with intensified induction chemotherapy, surgery followed by high-dose chemotherapy consolidation with autologous hematopoietic stem cell support, external-beam radiotherapy, and treatment of minimal residual disease with retinoids. Such aggressive treatment has increased the response rate; nevertheless, a significant proportion of patients remains resistant to induction treatment. Of those patients whose disease responds fully, more than 50% will relapse after consolidation (*2*). Overall, the long-term cure rate is less than 25%–30% (*3,4*).

Several diagnostic modalities are applied to define disease status in these patients. CT or MRI is used to assess the extent of the primary tumor and to detect any vascular or other vital organ encasement and contiguous or distant nodal metastases. MRI is the preferred modality for assessment of spinal canal involvement (*5,6*). ^{123}I-metaiodobenzylguanidine (^{123}I-MIBG) scintigraphy is the nuclear imaging method of choice for neuroblastoma, being valuable for diagnosis, staging, and response assessment. ^{123}I-MIBG scintigraphy has shown high diagnostic accuracy at initial staging, especially for the detection of osteomedullary lesions, and it subsequently provides an indispensable tool for the identification of residual, recurrent, or occult disease (*5–8*). The extent of ^{123}I-MIBG–positive disease before, during, and after treatment has been shown to correlate with event-free and overall survival (*9*).

^{18}F-FDG PET/CT is an established modality for many adult cancer types; however, its clinical role in pediatric malignancy is less well addressed (*10,11*). Lymphomas, primary brain neoplasms, and sarcomas have been most frequently studied, whereas few studies have investigated the use of ^{18}F-FDG in neuroblastoma (*12–15*). Among these studies, initial reports showed tumor avidity for ^{18}F-FDG (*14*), and it was later proposed that ^{18}F-FDG PET could be

Received Sep. 13, 2010; revision accepted Jan. 7, 2011.
For correspondence or reprints contact: Jamshed B. Bomanji, Institute of Nuclear Medicine, University College London Hospital, 235 Euston Rd., London, U.K. NW1 2BU.
E-mail: jamshed.bomanji@uclh.nhs.uk

implemented as the sole imaging modality to assess disease progression (*12*). However, the accuracy and clinical role of this technique have not been defined, especially for high-risk patients in whom determination of disease status is critical to gauge therapeutic management. Beyond disease detection, it is not known whether ^{18}F-FDG PET is able to provide prognostic information or whether the imaging results correlate with survival; similarly, it is unclear whether, within this cohort of patients with high-risk, aggressive tumors, ^{18}F-FDG PET can identify those who are likely to fail multimodality treatment.

The purpose of this study was to evaluate the diagnostic performance and prognostic significance of ^{18}F-FDG PET/CT in comparison with ^{123}I-MIBG imaging in patients with high-risk neuroblastoma.

MATERIALS AND METHODS

Study Population

Our prospective study considered 28 patients (Table 1; 16 male and 12 female patients; age range, 2–45 y; median age, 7.5 y) with high-risk, histologically proven neuroblastoma. Patients were referred to University College London Hospital, for combined high-dose ^{131}I-MIBG and topotecan treatment (Metaiodobenzylguanidine And Topotecan In Neuroblastoma protocol (*16*)) because of disease refractory to induction treatment (43%) or disease relapse after consolidation (57%). All of the patients had stage IV neuroblastoma: 25 with bone–bone marrow disease, 2 with liver involvement, and 1 with distant nodal metastases. Each patient underwent a pair of ^{18}F-FDG and ^{123}I-MIBG scans, performed within 2 wk before treatment. Scans were acquired from November 2004 until October 2008. Detailed informed parental or, when appropriate, patient consent was obtained according to the Declaration of Helsinki.

Imaging Protocols

PET/CT studies were performed using a dedicated combined Discovery (GE Healthcare) PET/CT scanner; whole-body examinations were performed with the patient supine. Images were acquired 50–75 min after injection of ^{18}F-FDG (5.5–7.7 MBq/kg), with a maximum dosage of 440 MBq. CT data were acquired using the four 3.75-mm detectors, a pitch of 1.5, and 5-mm colli-

TABLE 1
Patients' Demographic Data, Skeletal Scores, SUV_{max} of Most Intense Lesion per Patient, and Survival Data

Patient no.	Age (y)	Sex	Disease status	^{18}F-FDG skeletal scores	^{123}I-MIBG skeletal scores	SUV_{max}	Survival (y)	Event
1	11	M	Relapse	1	8	3.3	2.21	Death
2	7	F	Relapse	19	12	4.7	0.46	Death
3	15	F	Refractory	0	2	PET-negative†	0.83	Death
4	11	M	Relapse	2	2	3.8	2.83	Death
5	11	F	Relapse	0	6	5	2.03	Alive*
6	45	M	Relapse	4	4	4.8	3.03	Alive*
7	5	F	Relapse	0	11	PET-negative†	3.50	Alive at cutoff date
8	6	M	Refractory	17	17	4.9	0.56	Death
9	4	M	Refractory	6	12	1.5	2.12	Alive*
10	6	M	Relapse	1	3	2.4	2.57	Death
11	4	F	Relapse	0	9	PET-negative†	0.97	Alive*
12	19	M	Relapse	8	3	6	1.64	Death
13	9	M	Relapse	21	25	4.7	0.40	Death
14	7	F	Relapse	6	4	3.1	1.06	Death
15	4	M	Relapse	13	13	14	0.30	Death
16	8	M	Relapse	16	18	4.5	0.40	Death
17	8	F	Relapse	2	2	11.3	1.32	Death
18	6	M	Refractory	0	4	PET-negative†	1.13	Death
19	12	F	Relapse	1	1	9.8	0.44	Death
20	4	F	Refractory	11	5	7.9	0.27	Death
21	3	M	Refractory	11	7	2.3	0.73	Death
22	2	M	Refractory	0	0	2.6	1.25	Alive at cutoff date
23	3	F	Refractory	2	2	1.5	1.13	Alive at cutoff date
24	21	M	Refractory	0	0	10	0.54	Death
25	6	F	Refractory	10	14	5.6	0.95	Alive*
26	15	M	Refractory	0	0	1.4	1.01	Alive at cutoff date
27	8	M	Refractory	0	0	2.5	0.86	Alive*
28	24	F	Relapse	12	10	8	2.12	Alive at cutoff date

*Alive, but censored at earlier date than cutoff date.
†No SUV_{max} was measured.

mation. The CT exposure factors were 120–140 kVp and 80 mA. While patient position was maintained, a whole-body PET emission scan was acquired in 2-dimensional mode (5 min per bed position) and covered an area identical to that covered by CT. PET images were reconstructed using CT data for attenuation correction. Transaxial PET emission images of 4.3 × 4.3 × 4.25 mm were reconstructed using ordered-subsets expectation maximization, with 2 iterations and 28 subsets.

^{123}I-MIBG scans were obtained at 4 and 24 h after injection of ^{123}I-MIBG (5.20 MBq/kg), with a maximum dose of 370 MBq. All patients received thyroid blockage with potassium perchlorate or potassium iodide before and for 2 d after ^{123}I-MIBG administration. Anterior and posterior whole-body images were acquired. After initial review, planar whole-body images were supplemented with spot views or SPECT/CT of the chest and abdomen, if deemed necessary for anatomic localization of the lesion or clarification of equivocal findings. When necessary, sedation was used in accordance with guidelines before ^{18}F-FDG PET/CT or ^{123}I-MIBG imaging to ensure patient immobilization and adequate image quality.

Image Analysis

All studies were reviewed by 2 nuclear medicine physicians in consensus. For each single study (either ^{18}F-FDG PET/CT or ^{123}I-MIBG imaging), the presence or absence of disease was recorded separately for the soft-tissue compartment (primary mass, nodal, and liver metastases) and bone–bone marrow compartment. The number of involved soft-tissue regions (primary site, nodal sites, pleura–lung, and liver) detected by each modality was recorded.

For ^{18}F-FDG PET/CT interpretation, any focal, superior-to-background ^{18}F-FDG uptake in the primary mass, lymph nodes, liver, or skeleton was interpreted as positive or abnormal. Patchy inhomogeneous ^{18}F-FDG uptake in the bone marrow, especially in the absence of recent chemotherapy or hematopoietic stimulating factors, was interpreted as positive for bone marrow infiltration. The maximum standardized uptake values (SUV_{max}) were recorded for the most intense soft-tissue and bone–bone marrow lesions per patient, after manual application of regions of interest in the transaxial attenuation-corrected PET slices, around the pixels demonstrating the greatest accumulation of ^{18}F-FDG.

^{123}I-MIBG and ^{18}F-FDG PET/CT scans were assigned extent scores for bone–bone marrow lesions according to a previously applied semiquantitative method (*17,18*). The skeleton was divided into 10 segments: calvarium, skull base–face, cervical–thoracic spine, lumbar–sacral spine, sternum–ribs–scapula, pelvis, upper arms, forearms–hands, upper legs, and lower legs–feet. For each segment, disease was scored as 0, no lesion; 1, 1 positive lesion; 2, 2 or more positive lesions but involvement of less than 50% of segment; or 3, involvement of more than 50% of segment. A total score for each scan was calculated by adding all segmental scores (maximum score of 30).

At the end, each pair of scans was assigned a qualitative characterization: "^{18}F-FDG better than ^{123}I-MIBG" (Fig. 1), "^{18}F-FDG equivalent to ^{123}I-MIBG" (Fig. 2), or "^{18}F-FDG inferior to ^{123}I-MIBG" (Fig. 3). For this grouping, interpreters took into account 2 integrated factors: the extent of the disease identified—that is, the number and distribution of involved regions—and the intensity of positive lesions (qualitative estimation of tumor-to-background ratios) on each tracer imaging. The liver (*14,18*) or an area free of disease, if the liver was involved, was used as background to estimate the intensity of lesions.

Survival Analysis

Overall survival was calculated from time of imaging to death or last examination (cutoff date for analysis, August 1, 2009), according to the Kaplan–Meier method. Univariate Cox regression analysis was applied to check for the prognostic significance of the following factors: age, ^{123}I-MIBG and ^{18}F-FDG skeletal scores, ^{123}I-MIBG and ^{18}F-FDG–positive soft-tissue regions, SUV_{max} (of the most ^{18}F-FDG–avid lesion in each patient), and ^{123}I-MIBG–^{18}F-FDG paired scan characterization ("^{18}F-FDG better than ^{123}I-MIBG" and "^{18}F-FDG equivalent to ^{123}I-MIBG" vs. "^{18}F-FDG inferior to ^{123}I-MIBG" as reference level). Analysis was performed using STATA software (version 10; StataCorp).

RESULTS

Image Analysis

^{123}I-MIBG imaging was positive in all 28 patients, whereas ^{18}F-FDG PET/CT was positive in 24 of 28, corresponding to an 86% per-patient sensitivity of ^{18}F-FDG for neuroblastoma detection.^{18}F-FDG missed 4 cases of disease in the soft tissue and 5 cases in the bone–bone marrow compartment, all of which were positive on ^{123}I-MIBG, whereas only 1 case of soft-tissue compartment disease was positive on ^{18}F-FDG and negative on ^{123}I-MIBG. ^{123}I-MIBG was superior to ^{18}F-FDG in both soft-tissue and bone–bone marrow compartments; however, this difference was not statistically significant (McNemar test; $P = 0.375$ and 0.063, respectively; Tables 2 and 3).

A total of 50 positive soft-tissue regions were identified in the whole study group, 32 (64%) of which were positive on both ^{18}F-FDG and ^{123}I-MIBG. Nonconcordant regions that were ^{123}I-MIBG–positive/^{18}F-FDG–negative (10/50 [20%]) were marginally more frequent than ^{123}I-MIBG–negative/^{18}F-FDG–positive regions (8/50 [16%]) ($\chi 2$ test, $P = 0.8$). Mean ^{123}I-MIBG skeletal extent scores (6.9 ± 1.2 SE) in the whole study group were not significantly different from respective ^{18}F-FDG scores (5.8 ± 1.3 SE)

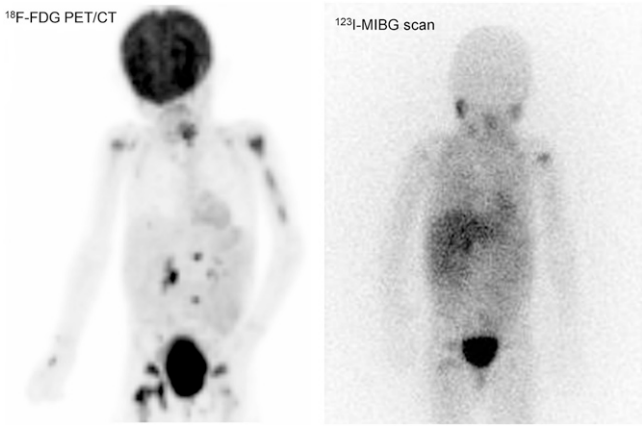

FIGURE 1. ^{18}F-FDG PET/CT scan (maximum-intensity projection) in 4-y-old girl shows more extensive and pronounced bone–bone marrow disease in humeri, spine, pelvis, and femora than does ^{123}I-MIBG scan (planar). Both modalities were negative for soft-tissue compartment and positive for the bone–bone marrow compartment. This pair of scans was characterized as showing better performance for ^{18}F-FDG than for ^{123}I-MIBG.

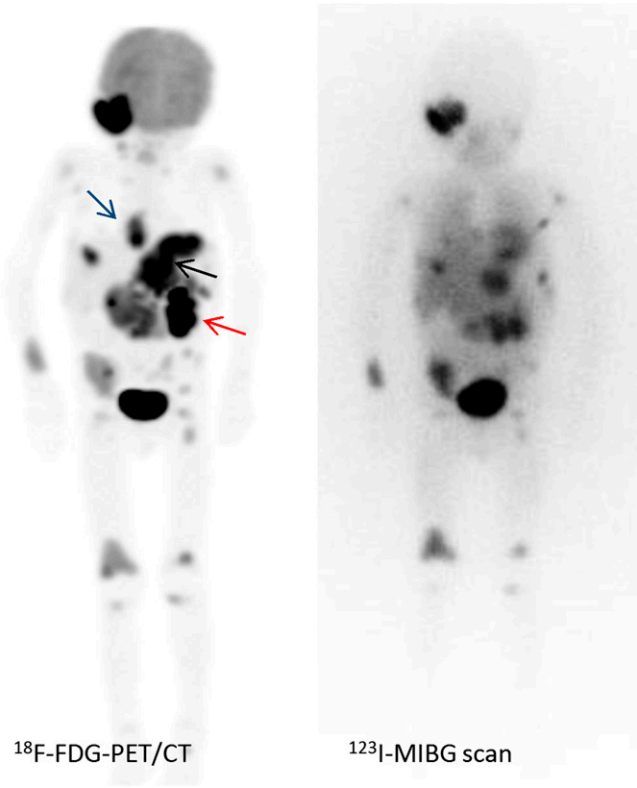

FIGURE 2. ^{18}F-FDG PET/CT (maximum-intensity projection) and ^{123}I-MIBG (anterior planar) scans of 4-y-old boy with extensive stage IV neuroblastoma. There are multiple bone–bone marrow lesions in skull (right temporal bone, with soft-tissue component), ribs, pelvis, and extremities, which were avid on images obtained with both tracers (^{123}I-MIBG and ^{18}F-FDG skeletal scores of 13). There are soft-tissue masses in posterior mediastinum (blue arrow) and abdomen (black arrow), causing obstruction of left kidney (red arrow). This pair of scans was characterized as showing equivalence between ^{18}F-FDG and ^{123}I-MIBG.

(paired t test, $P = 0.22$). Mean SUV_{max} was 5.6 ± 3.2 SD for the soft-tissue lesions and 5.1 ± 3.6 SD for the bone–bone marrow lesions. Patients' skeletal scores and SUV_{max} are shown in Table 1.

Eight patients had skull lesions detected by ^{123}I-MIBG imaging; in 2, the lesions had a large soft-tissue component and were visible on ^{18}F-FDG PET/CT as well, whereas the other 6 lesions were missed by ^{18}F-FDG. In 5 of these patients, these results had no implications for staging—^{18}F-FDG was positive for the bone–bone marrow compartment anyway. In the other patient, ^{18}F-FDG missed both skull involvement and bone–bone marrow disease detected by ^{123}I-MIBG. The 2 cases of liver involvement were positive on ^{123}I-MIBG scans, and 1 of them showed avidity for ^{18}F-FDG as well.

Qualitative paired comparisons revealed ^{18}F-FDG to be better than ^{123}I-MIBG in mapping tumor load in 4 of 28 patients (14%; 95% confidence interval [CI], 6%–31%). These cases included 2 in which ^{18}F-FDG detected more soft-tissue lesions and 2 in which ^{18}F-FDG better delineated the bone–bone marrow component of the disease (Fig. 1). In 12 patients (43%; 95% CI, 27%–61%), ^{18}F-FDG was inferior to ^{123}I-MIBG. These cases comprised 3 in which ^{18}F-FDG was worse in depicting disease in the soft-tissue compartment, 4 in which ^{18}F-FDG was worse in depicting disease in the bone–bone marrow compartment, and 5 in which the performance of ^{18}F-FDG was worse in both compartments (Fig. 3). In the remaining 12 patients (43%; 95% CI, 27%–61%), there was no significant discordance between the 2 modalities, and the paired scans were characterized as equivalent (Fig. 2).

Survival Analysis

Median observation time from imaging was 1.03 y (range, 0.27–3.5 y). Seventeen patients (61%) died during the observation period, and Kaplan–Meier median survival time was 1.32 y. The Kaplan–Meier estimate of the 3-y overall survival of the group was 17% (95% CI, 3%–41%). Cox regression analysis showed that compared with ^{123}I-MIBG (paired ^{123}I-MIBG–^{18}F-FDG scan characterization) (Fig. 4), ^{18}F-FDG uptake pattern, tumoral ^{18}F-FDG uptake (SUV_{max}) (Fig. 5), and ^{18}F-FDG skeletal extent score (Fig. 6) were significant factors associated with decreased survival (Table 4).

DISCUSSION

Ours is one of the first prospective studies to directly compare the diagnostic performance of ^{18}F-FDG PET/CT with ^{123}I-MIBG imaging in high-risk neuroblastoma. The

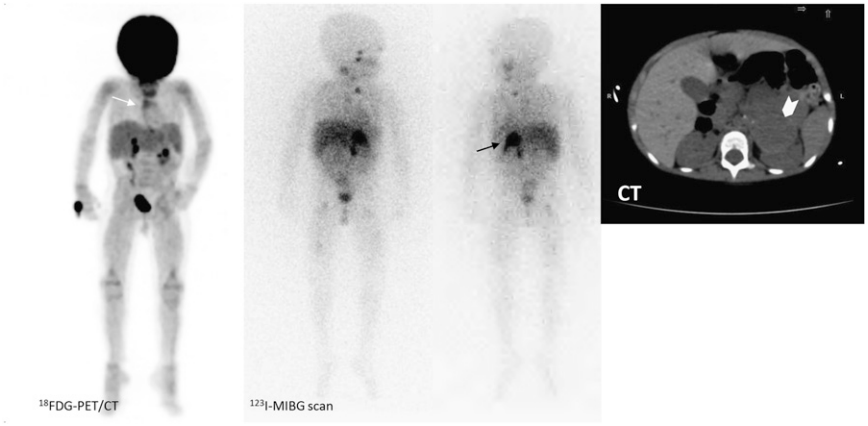

FIGURE 3. ^{18}F-FDG PET/CT (maximum-intensity projection) and ^{123}I-MIBG (anterior and posterior planar) scans of 3-y-old boy with stage IV neuroblastoma. There is extensive ^{123}I-MIBG–avid disease in bone–bone marrow and ^{123}I-MIBG–avid (black arrow) left adrenal mass (CT image; white arrowhead). ^{18}F-FDG PET shows intense tracer uptake only in sternum (white arrow), in keeping with bone–bone marrow disease. This pair of scans was characterized as showing ^{18}F-FDG to be inferior to ^{123}I-MIBG.

TABLE 2
^{123}I-MIBG and ^{18}F-FDG Imaging Results, per Patient, in Soft-Tissue Compartment

	^{18}F-FDG		
^{123}I-MIBG	Positive	Negative	Total
Positive	14	4	18 (64%)
Negative	1	9	10 (36%)
Total	15 (54%)	13 (46%)	28 (100%)

Percentages within parentheses refer to total number of patients. McNemar test *P* value was 0.375.

results show good per-patient sensitivity (86%) of ^{18}F-FDG PET/CT for neuroblastoma detection; however, ^{123}I-MIBG imaging was, overall, superior in mapping the extent of the disease. Most previous studies, though limited, are in accordance with our results. Initially, Shulkin et al. reported tumoral ^{18}F-FDG avidity in 16 of 17 patients, yet in most cases MIBG was rated superior for tumor delineation (*14*). In a retrospective study of 85 paired scans in 40 stage IV patients, ^{123}I-MIBG was superior to ^{18}F-FDG PET (*13*). Similarly, ^{123}I-MIBG was more sensitive overall and for bone lesions than ^{18}F-FDG PET in patients of the New Approaches to Neuroblastoma Therapy (NANT) trial, assessed before ^{131}I-MIBG therapy (*15*). Unlike these and our results, 1 study of 51 high-risk subjects showed ^{18}F-FDG PET to be better than MIBG for detection of both extracranial osteomedullary and soft-tissue lesions (*12*).

The main advantage of ^{123}I-MIBG over ^{18}F-FDG was its superiority in depicting clearly the bone–bone marrow component of the disease (Table 3), because uptake of ^{123}I-MIBG was not confounded by bone marrow activation due to previously applied therapies. Our finding is supported by results from previous studies (*13,14*). In contrast, ^{18}F-FDG may exhibit physiologic accumulation in the bone marrow regardless of whether it is infiltrated, resulting in lower accuracy for detection of bone–bone marrow disease. ^{18}F-FDG was inferior in detecting skull lesions, unless these demonstrated a considerable soft-tissue component, mainly because of the adjacent high physiologic ^{18}F-FDG

TABLE 3
^{123}I-MIBG and ^{18}F-FDG Imaging Results, per Patient, in Bone–Bone Marrow Compartment

	^{18}F-FDG		
^{123}I-MIBG	Positive	Negative	Total
Positive	19	5	24 (86%)
Negative	0	4	4 (14%)
Total	19 (68%)	9 (32%)	28 (100%)

Percentages within parentheses refer to total number of patients. McNemar test *P* value was 0.063.

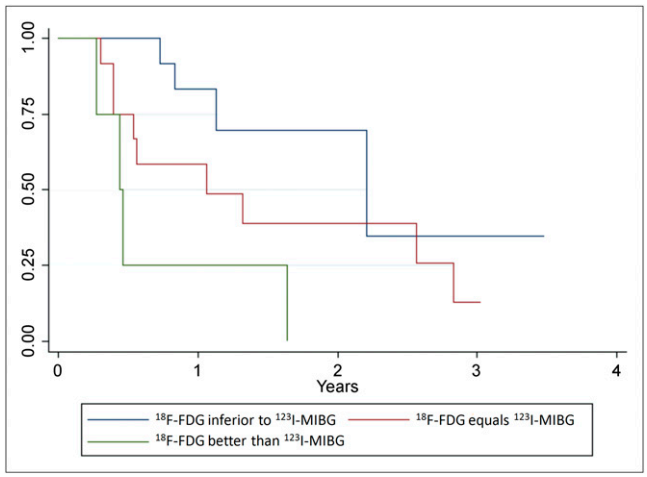

FIGURE 4. Kaplan–Meier survival curves of 3 groups of patients: "^{18}F-FDG better than ^{123}I-MIBG" (green line) and "^{18}F-FDG equivalent to ^{123}I-MIBG" (red line) vs. "^{18}F-FDG inferior to ^{123}I-MIBG" (blue line).

activity in the brain cortex. Although it has been hypothesized that ^{18}F-FDG could be better in detecting liver lesions (*5,19*) because of physiologic ^{123}I-MIBG distribution in the liver, this hypothesis was not confirmed by our results.

Beyond disease detection, ^{18}F-FDG PET/CT had significant prognostic implications in high-risk neuroblastoma patients undergoing ^{131}I-MIBG treatment. Tumoral metabolic activity (SUV_{max}) and extent of ^{18}F-FDG–avid bone–bone marrow disease (^{18}F-FDG skeletal scores) were identified as poor prognostic factors associated with decreased survival (Table 4; Figs. 5 and 6). A pattern of increased ^{18}F-FDG activity, surpassing tumoral avidity for ^{123}I-MIBG, corresponded to more aggressive disease and worse outcome (Table 4; Fig. 4). It is unknown whether this pattern mirrors neuroblastoma cell dedifferentiation. In a significant number of preclinical and clinical studies, ^{18}F-FDG uptake was found to correlate with high proliferative activity, cellular dedifferentiation, and aggressive behavior of neuroendo-

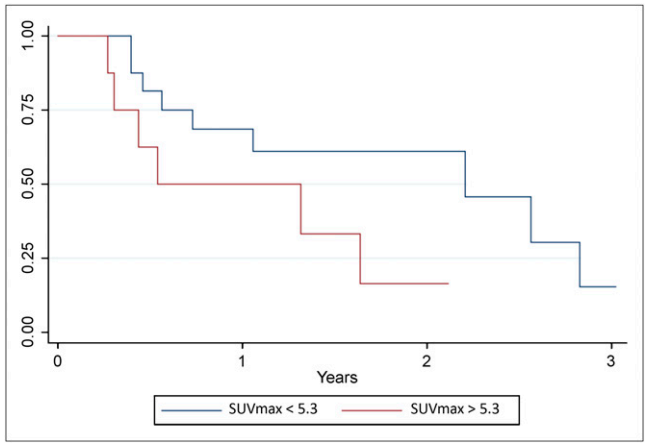

FIGURE 5. Kaplan–Meier survival curves of patients whose most intense lesion had a $SUV_{max} > 5.3$ (red line) vs. others with $SUV_{max} < 5.3$ (blue line). Mean SUV_{max} was selected as cutoff value.

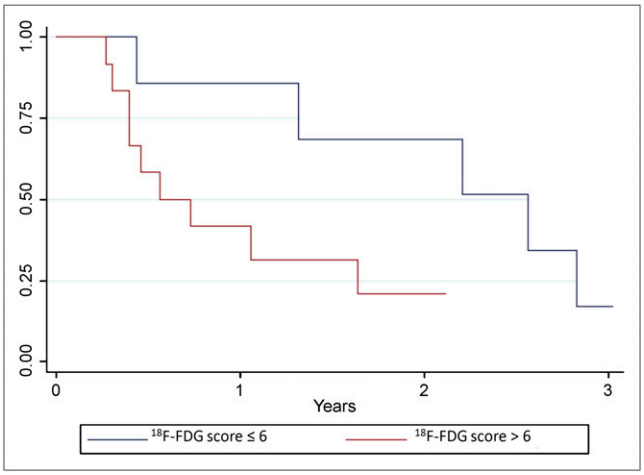

FIGURE 6. Kaplan–Meier survival curves of patients with ^{18}F-FDG skeletal score of >6 (red line) vs. skeletal score of ≤6 (blue line). Mean ^{18}F-FDG skeletal score was selected as cutoff value.

crine tumors (*20,21*); however, preclinical models have failed to verify any association between ^{18}F-FDG and neuroblastoma proliferation (*22*). MIBG is taken up by the neuroblastoma cells because of a specific noradrenaline transporter mechanism (*23*), but its uptake within tumors is highly variable and has not been found to correlate with neuroblastoma differentiation (*24*). There is a need for preclinical studies to clarify whether there is a pattern of unfavorable histology, with neuroblast cellular dedifferentiation correlating with increased ^{18}F-FDG activity and lesser MIBG uptake.

Our results showed a nonsignificant association of ^{123}I-MIBG imaging parameters (skeletal scoring systems and positive soft-tissue regions) with survival, probably reflecting our specific group selection of heavily pretreated patients with relapsed or refractory disease. In a similar group of 49 patients, Messina et al. reported that ^{123}I-MIBG scores showed high reproducibility and correlated with therapeutic response but were not associated with survival outcome (*18*). In a different clinical setting, postinduction ^{123}I-MIBG score was significantly associated with outcome: those with a score less than 3 had a 4-y event-free survival rate of 58% ± 11%, as compared with a survival rate of 0% in those with a score more than 3 (*17*). In a large study of 113 stage IV patients, the presence of ^{123}I-MIBG–positive metastatic disease after 4 cycles of induction was related to decreased 3-y overall survival: 49.8% ± 6.1% vs. 65% ± 7.3% when ^{123}I-MIBG was negative for metastatic disease (*9*). It seems that ^{123}I-MIBG can predict outcome in initial treatment evaluation (after induction) but not later in patients with relapsed or refractory disease, who carry a dramatically poor prognosis.

The main limitation of this study is that we did not incorporate parameters (e.g., dosimetry, response evaluation) of subsequent ^{131}I-MIBG treatment, or details of any other subsequent treatments, into the survival analysis. These factors could considerably affect total survival time, and to evaluate their effect we would require data from a larger cohort of patients to obtain adequate power and analyze with a multivariable model to exclude potential confounders. Such analysis was beyond the scope of the planned comparison of the 2 modalities and will be the subject of a subsequent study. Second, our imaging results were not validated against a standard reference method: obtaining tissue histology from all sites was not feasible or ethical and there is no imaging gold standard in the evaluation of neuroblastoma patients. Therefore, the effect of this inherent limitation on accuracies of imaging modalities cannot be correctly determined; the sensitivity of ^{18}F-FDG PET/CT could have been overestimated because of false-positive lesions, especially in the bone–bone marrow compartment. Another limitation is the referral bias: we evaluated MIBG-avid neuroblastoma patients treated subsequently with ^{131}I-MIBG; therefore, extending our conclusions to all high-risk neuroblastoma patients (MIBG-avid and -nonavid) should be done with caution. Finally, the use of ^{18}F-FDG PET/CT in addition to ^{123}I-MIBG scintigraphy at initial staging in all neuroblastoma patients (including those at high risk) requires prospective evaluation.

TABLE 4
Results of Univariate Cox Regression Analysis

Variable	*P*	Hazard ratio*	95% CI of hazard ratio
SUV_{max}	0.013	1.23	1.04–1.45
^{18}F-FDG better than ^{123}I-MIBG	0.009	6.67	1.62–27.55
^{18}F-FDG equivalent to ^{123}I-MIBG vs. ^{18}F-FDG inferior to ^{123}I-MIBG (reference level)	0.17	2.3	0.69–7.62
	Overall 0.03†		
^{18}F-FDG skeletal score	0.002	1.15	1.05–1.25
Age	0.25		
^{123}I-MIBG skeletal score	0.27		
^{123}I-MIBG–positive soft-tissue lesions	0.7		
^{18}F-FDG–positive soft-tissue lesions	0.5		

*Hazard ratios of nonsignificant factors are not shown.
†*P* value of overall likelihood ratio test.

CONCLUSION

^{18}F-FDG PET/CT cannot replace ^{123}I-MIBG in high-risk neuroblastoma, mainly because of its limitation in identifying bone–bone marrow infiltration. ^{18}F-FDG PET/CT could be useful in the evaluation of a small proportion (less than 10%) of neuroblastoma patients who do not accumulate ^{123}I-MIBG or in cases in which it is suspected that the extent of disease exceeds that depicted with ^{123}I-MIBG (*13,14,19*). Tumoral ^{18}F-FDG avidity was associated with an earlier adverse outcome within this cohort of patients with a poor prognosis undergoing ^{131}I-MIBG therapy. The practical incorporation of ^{18}F-FDG PET/CT in treatment decision making would, however, require the development of novel effective treatments (*25*). In such a setting, ^{18}F-FDG PET/CT could aid in identifying patients for whom a more aggressive treatment strategy would be required.

DISCLOSURE STATEMENT

The costs of publication of this article were defrayed in part by the payment of page charges. Therefore, and solely to indicate this fact, this article is hereby marked "advertisement" in accordance with 18 USC section 1734.

ACKNOWLEDGMENTS

We thank Anastasios Boutsiadis and Xanthi Pedeli, biostatisticians, for statistical advice. This work was undertaken at the University College London Hospital, which receives a proportion of financial support from the U.K. Department of Health's NIHR Comprehensive Biomedical Research Centres funding scheme and from Cancer Research, United Kingdom.

REFERENCES

1. Maris JM, Hogarty MD, Bagatell R, Cohn SL. Neuroblastoma. *Lancet.* 2007;369:2106–2120.
2. Matthay KK, Villablanca JG, Seeger RC, et al. Treatment of high-risk neuroblastoma with intensive chemotherapy, radiotherapy, autologous bone marrow transplantation, and 13-cis-retinoic acid. Children's Cancer Group. *N Engl J Med.* 1999;341:1165–1173.
3. Pearson AD, Pinkerton CR, Lewis IJ, Imeson J, Ellershaw C, Machin D. High-dose rapid and standard induction chemotherapy for patients aged over 1 year with stage 4 neuroblastoma: a randomised trial. *Lancet Oncol.* 2008;9:247–256.
4. Zage PE, Kletzel M, Murray K, et al. Outcomes of the POG 9340/9341/9342 trials for children with high-risk neuroblastoma: a report from the Children's Oncology Group. *Pediatr Blood Cancer.* 2008;51:747–753.
5. Howman-Giles R, Shaw PJ, Uren RF, Chung DK. Neuroblastoma and other neuroendocrine tumors. *Semin Nucl Med.* 2007;37:286–302.
6. Kushner BH. Neuroblastoma: a disease requiring a multitude of imaging studies. *J Nucl Med.* 2004;45:1172–1188.
7. Kushner BH, Kramer K, Modak S, Cheung NK. Sensitivity of surveillance studies for detecting asymptomatic and unsuspected relapse of high-risk neuroblastoma. *J Clin Oncol.* 2009;27:1041–1046.
8. Vik TA, Pfluger T, Kadota R, et al. ^{123}I-mIBG scintigraphy in patients with known or suspected neuroblastoma: results from a prospective multicenter trial. *Pediatr Blood Cancer.* 2009;52:784–790.
9. Schmidt M, Simon T, Hero B, Schicha H, Berthold F. The prognostic impact of functional imaging with ^{123}I-mIBG in patients with stage 4 neuroblastoma >1 year of age on a high-risk treatment protocol: results of the German Neuroblastoma Trial NB97. *Eur J Cancer.* 2008;44:1552–1558.
10. Jadvar H, Connolly LP, Fahey FH, Shulkin BL. PET and PET/CT in pediatric oncology. *Semin Nucl Med.* 2007;37:316–331.
11. Kleis M, Daldrup-Link H, Matthay K, et al. Diagnostic value of PET/CT for the staging and restaging of pediatric tumors. *Eur J Nucl Med Mol Imaging.* 2009;36:23–36.
12. Kushner BH, Yeung HW, Larson SM, Kramer K, Cheung NK. Extending positron emission tomography scan utility to high-risk neuroblastoma: fluorine-18 fluorodeoxyglucose positron emission tomography as sole imaging modality in follow-up of patients. *J Clin Oncol.* 2001;19:3397–3405.
13. Sharp SE, Shulkin BL, Gelfand MJ, Salisbury S, Furman WL. ^{123}I-MIBG scintigraphy and ^{18}F-FDG PET in neuroblastoma. *J Nucl Med.* 2009;50:1237–1243.
14. Shulkin BL, Hutchinson RJ, Castle VP, Yanik GA, Shapiro B, Sisson JC. Neuroblastoma: positron emission tomography with 2-[fluorine-18]-fluoro-2-deoxy-D-glucose compared with metaiodobenzylguanidine scintigraphy. *Radiology.* 1996;199:743–750.
15. Taggart DR, Han MM, Quach A, et al. Comparison of iodine-123 metaiodobenzylguanidine (MIBG) scan and [^{18}F]fluorodeoxyglucose positron emission tomography to evaluate response after iodine-131 MIBG therapy for relapsed neuroblastoma. *J Clin Oncol.* 2009;27:5343–5349.
16. Gaze MN, Chang YC, Flux GD, Mairs RJ, Saran FH, Meller ST. Feasibility of dosimetry-based high-dose ^{131}I-meta-iodobenzylguanidine with topotecan as a radiosensitizer in children with metastatic neuroblastoma. *Cancer Biother Radiopharm.* 2005;20:195–199.
17. Katzenstein HM, Cohn SL, Shore RM, et al. Scintigraphic response by ^{123}I-metaiodobenzylguanidine scan correlates with event-free survival in high-risk neuroblastoma. *J Clin Oncol.* 2004;22:3909–3915.
18. Messina JA, Cheng SC, Franc BL, et al. Evaluation of semi-quantitative scoring system for metaiodobenzylguanidine (mIBG) scans in patients with relapsed neuroblastoma. *Pediatr Blood Cancer.* 2006;47:865–874.
19. Colavolpe C, Guedj E, Cammilleri S, Taieb D, Mundler O, Coze C. Utility of FDG-PET/CT in the follow-up of neuroblastoma which became MIBG-negative. *Pediatr Blood Cancer.* 2008;51:828–831.
20. Adams S, Baum RP, Hertel A, Schumm-Drager PM, Usadel KH, Hor G. Metabolic (PET) and receptor (SPET) imaging of well- and less well-differentiated tumours: comparison with the expression of the Ki-67 antigen. *Nucl Med Commun.* 1998;19:641–647.
21. Kayani I, Bomanji JB, Groves A, et al. Functional imaging of neuroendocrine tumors with combined PET/CT using ^{68}Ga-DOTATATE (DOTA-DPhe1,Tyr3-octreotate) and ^{18}F-FDG. *Cancer.* 2008;112:2447–2455.
22. Krieger-Hinck N, Gustke H, Valentiner U, et al. Visualisation of neuroblastoma growth in a Scid mouse model using [^{18}F]FDG and [^{18}F]FLT-PET. *Anticancer Res.* 2006;26(5A):3467–3472.
23. DuBois SG, Matthay KK. Radiolabeled metaiodobenzylguanidine for the treatment of neuroblastoma. *Nucl Med Biol.* 2008;35(suppl 1):S35–S48.
24. Brans B, Laureys G, Schelfhout V, et al. Activity of iodine-123 metaiodobenzylguanidine in childhood neuroblastoma: lack of relation to tumour differentiation in vivo. *Eur J Nucl Med.* 1998;25:144–149.
25. Wagner LM, Danks MK. New therapeutic targets for the treatment of high-risk neuroblastoma. *J Cell Biochem.* 2009;107:46–57.

JNM The Journal of NUCLEAR MEDICINE

^{18}F-FDG PET/CT and ^{123}I-Metaiodobenzylguanidine Imaging in High-Risk Neuroblastoma: Diagnostic Comparison and Survival Analysis

Nikolaos D. Papathanasiou, Mark N. Gaze, Kevin Sullivan, Matthew Aldridge, Wendy Waddington, Ahmad Almuhaideb and Jamshed B. Bomanji

J Nucl Med. 2011;52:519-525.
Published online: March 18, 2011.
Doi: 10.2967/jnumed.110.083303

The Journal of Nuclear Medicine is published monthly.
SNMMI | Society of Nuclear Medicine and Molecular Imaging
1850 Samuel Morse Drive, Reston, VA 20190.
(Print ISSN: 0161-5505, Online ISSN: 2159-662X)

SNMMI SOCIETY OF NUCLEAR MEDICINE AND MOLECULAR IMAGING